AIP | Applied Physics Letters

Continuous optoelectrowetting for picoliter droplet manipulation

P. Y. Chiou, Sung-Yong Park, and Ming C. Wu

Citation: Applied Physics Letters **93**, 221110 (2008); doi: 10.1063/1.3039070
View online: http://dx.doi.org/10.1063/1.3039070
View Table of Contents: http://scitation.aip.org/content/aip/journal/apl/93/22?ver=pdfcov
Published by the AIP Publishing

Continuous optoelectrowetting for picoliter droplet manipulation

P. Y. Chiou,[1] Sung-Yong Park,[1,a)] and Ming C. Wu[2]
[1]*Department of Mechanical and Aerospace Engineering, University of California at Los Angeles (UCLA), 48-121 ENG. IV, 420 Westwood Plaza, Los Angeles, California 90095-1597, USA*
[2]*Department of Electrical Engineering and Computer Sciences, University of California, Berkeley, California 94720, USA and Berkeley Sensor & Actuator Center, University of California, Berkeley, California 94720, USA*

(Received 19 September 2008; accepted 10 November 2008; published online 4 December 2008)

We report on a continuous optoelectrowetting mechanism enabling continuous high spatial resolution optical modulation of electrowetting effect on a featureless planar photoconductive amorphous silicon surface. Dynamically patterned "virtual electrode" switches voltage between the amorphous silicon layer and the dielectric layer for contact angle modulation. This device is particularly attractive for manipulating picoliter droplets. We have experimentally demonstrated trapping and moving of 10 and 50 pl droplets at a speed of 1 mm/s using a light beam. © *2008 American Institute of Physics*. [DOI: 10.1063/1.3039070]

Droplet based microfluidic devices have received a lot of interests recently because they eliminate the need for pumps and valves and minimize cross-contamination between samples. Several mechanisms have been proposed to drive liquid droplets in microscale. Droplet actuation mechanisms are versatile including Marangoni effect,[1] photosensitive surface treatment,[2] surface acoustic wave,[3] dielectrophoresis,[4,5] and electrowetting.[6–8] Among these mechanisms, electrowetting is one of the most effective methods due to its low electrical power consumption, easy implementation, and fast response. Optoelectrowetting is a mechanism that enables optical control of electrowetting with patterned optical images.[8–10] Optoelectrowetting is typically realized using a patterned electrode serially connected with a photoconductor. By illuminating this photoconductor, voltage used to activate electrowetting effect can be optically modulated. The minimum droplet size that can be manipulated is limited by the electrode size.

Here, we present a new concept to manipulate liquid droplets without pixilated electrodes. By using a single continuous optoelectrowetting (COEW) electrode, the liquid volume is determined by the spot size of a light beam. Picoliter droplet manipulation can be achieved by using a micron size light spot on the COEW surface.

The schematic of the COEW device is shown in Fig. 1. The bottom surface is a glass substrate coated with 0.2 μm Al layer, 5 μm amorphous silicon layer, 0.2 μm plasma-enhanced chemical-vapor deposition (PECVD) silicon oxide layer, and 0.05 μm Teflon layer subsequently. The top surface is a transparent conductive indium tin oxide (ITO) glass with a 0.2 μm PECVD silicon oxide layer and a 0.05 μm Teflon layer. An ac bias is applied between the two ITO electrodes. The droplet is sandwiched between the top and bottom electrodes separated by a photoresist spacer with a thickness of 10 μm.

The contact angle of a water droplet on a Teflon surface is 108°. Upon optical illumination, the photoconductivity of the amorphous silicon layer increases and shifts the voltage to the dielectric silicon dioxide and Teflon layers, which decreases the contact angle according to Lippman-Young's equation,[11]

$$\cos[\theta(V_i)] = \cos[\theta(0)] + \frac{1}{2}\frac{\varepsilon}{d\gamma_{LV}}V_i^2, \tag{1}$$

where V_i, d, ε, and γ_{LV} represent the voltage, the thickness, and the dielectric constant of the insulation layer, and the interfacial tension between liquid and vapor, respectively.

The resolution of light patterned virtual electrode is limited by the optical diffraction limit of the optical system due to the short ambipolar diffusion length of the light excited electron hole pairs in amorphous silicon.[12] This allows patterning of high spatial resolution of virtual electrodes for continuous and dynamic modulation of electrowetting area on a COEW surface without limited by the size of physical electrodes.

From the equivalent circuit model in Fig. 1(b), the total electrical impedance of the circuit is equal to

$$Z_{\text{total}} = \frac{R_{\text{asi}}}{1 + i\omega R_{\text{asi}} C_{\text{asi}}} + \frac{2}{i\omega C_{\text{oxide}}} + \frac{R_{\text{water}}}{1 + i\omega R_{\text{water}} C_{\text{water}}}, \tag{2}$$

where R_{asi} and C_{asi} are the resistance and capacitance of the amorphous Si, C_{oxide} is the capacitance of SiO_2, and R_{water} and C_{water} are the resistance and capacitance of the water layer. The voltage dropping across the dielectric layer for electrowetting modulation is calculated in Fig. 2. The con-

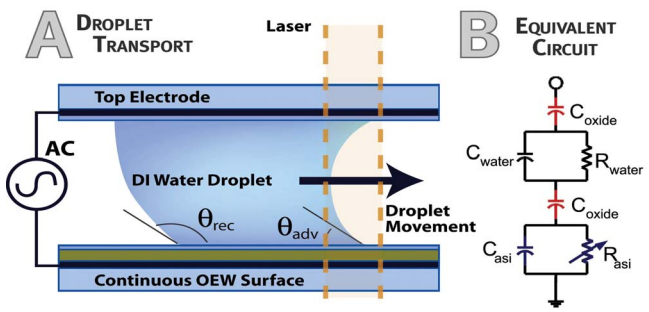

FIG. 1. (Color online) (a) Schematic illustrating the movement of a liquid droplet by an optical beam on a COEW surface. (b) Equivalent circuit model of the COEW device.

a)Electronic mail: spark5@ucla.edu.

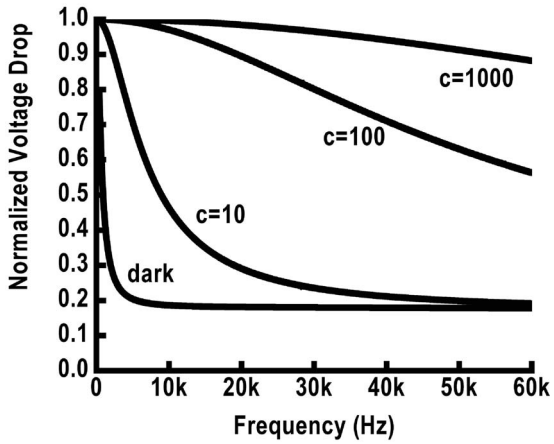

FIG. 2. The voltage drop across the insulation layer calculated from the equivalent circuit model in Fig. 1(b). The constant c represents the ratio of the peak photoconductivity to the dark conductivity.

stant c represents the ratio of the photoconductivity and the dark conductivity.

Optoelectrowetting devices are usually driven by an ac bias with an optimal frequency window. The optimum ac frequency window for the COEW is the between 10 and 30 kHz to ensure low dark voltage drop across the dielectric layer and low optical power actuation. In this range, more than 80% of the external voltage can be used to activate electrowetting when a light beam is strong enough to increase the photoconductivity 100 times ($c=100$). For frequencies below 1 kHz, most of the voltage drop occurs at the insulation layer even in the dark. In high frequency, stronger light intensity is required to fully switch the voltage to the insulation layer.

Figure 2 also shows that in the dark state ($c=0$), 20% of the external voltage drops across the silicon dioxide layer even for operation frequency higher than 5 kHz. To reduce the voltage drop across SiO_2 in the dark state, the photoconductor needs to be much thicker than the insulation layer. Currently, we use a 5 μm thick amorphous silicon layer and a total of 0.4 μm thick silicon dioxide layers.

The experimental setup for picoliter droplet manipulation is shown in Fig. 3(a). A 0.8 mW HeNe laser with a wavelength of 632 nm (Uniphase 1507) is used as the light source. The laser beam is steered by two orthogonal galvanometer scanning mirror set (Cambridge Inc.) and sent through a combination of a convex lens and a 10× objective lens to create a light spot with a diameter of 20 μm, providing an intensity of 254 W/cm^2. The optical absorption coefficient of amorphous Si at 632 nm is around 10^4/cm. Most of the transmitted light (~70%) is absorbed by the 5-μm-thick amorphous silicon layer. The motion of the droplets is captured by a charge coupled device camera.

Figures 3(b) and 3(c) present the trapping and moving of a 10 and a 50 pl droplets with size determined by the spacer thickness and the diameter of these droplets. We applied a 200 V_{pp} ac bias between the top and the bottom ITO electrodes in this experiment. The frequency of the ac bias is varied to verify the optimal frequency window predicted in the simulation. We found that between 10 and 30 kHz, the droplets are effectively moved or trapped by the optical beam. Below 1 kHz or above 180 kHz, the droplets do not respond to the laser beam, which matches well with our

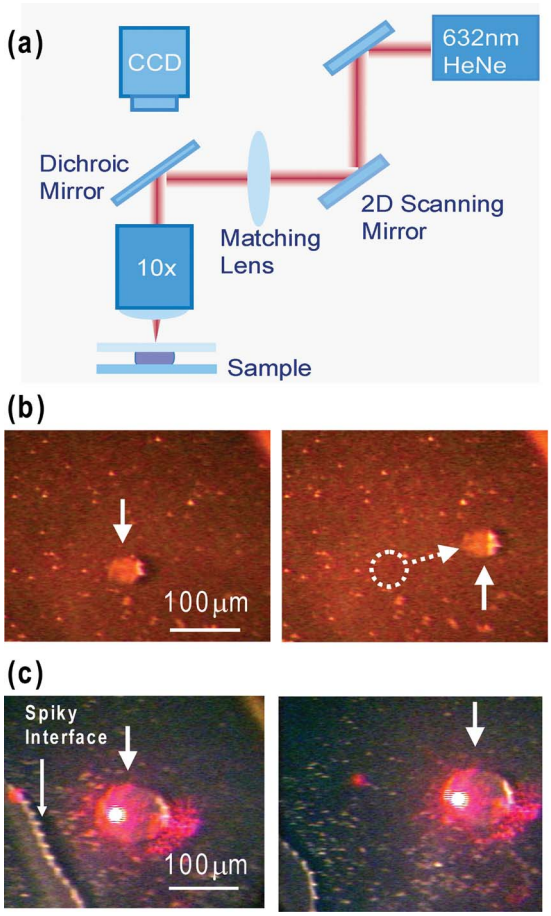

FIG. 3. (Color online) (a) Experimental setup of picoliter droplet manipulation. (b) Example of optical trapping and transporting of 10 pl droplet. (c) Example of transporting of a 50 pl droplet.

simulation. This also implies that the droplet movement is not due to photothermal heating of the amorphous silicon substrate. In fact, the light intensity required here is an order of magnitude lower than the minimum optical intensity used for thermal capillary actuation on an amorphous silicon substrate.[13]

One phenomenon that has been observed in our experiment is the oscillating droplet surface under ac bias as indicated in Fig. 3(b). This oscillation occurs even at areas without optical illumination. This effect results from the electric field existing in the air gap, as shown in Fig. 4. At areas covered with water droplets, the electric field inside a droplet is fully screened in 10 kHz ac frequency and the voltage

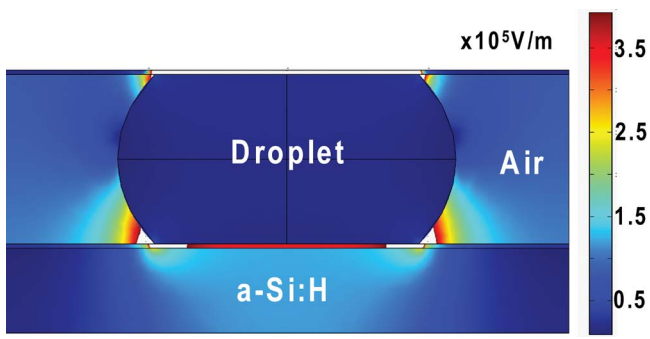

FIG. 4. (Color online) Simulated electric field distribution around a droplet without optical illumination.

either drops across the amorphous silicon layer or the dielectric layer. However, at areas without water coverage, most voltage drop across the air gap due to its large electrical impedance compared to the dielectric layer or the dark amorphous silicon layer. The difference in electric field inside and outside a droplet interface results in Maxwell stress on the liquid-air interface as well as near the three phase line, which can cause droplet oscillation in ac electrowetting as pointed out by Oh *et al.*[14] Since the force exists symmetrically around a droplet, it does not result in net droplet transport and could be utilized for rapid droplet mixing.[15]

COEW enables continuous optical modulation of electrowetting effect on a photoconductive featureless substrate for precise droplet manipulation and accurate addressing without limited by the pitch size of physical electrodes. We have demonstrated optically driven trapping and moving of droplets with volume of 10 and 50 pl. A moving speed as high as 1 mm/s has been observed by applying 200 V_{pp} ac bias with frequency between 10 and 30 kHz. By projecting patterned optical images, COEW should allow more complex droplet functions such as droplet injection from a reservoir, droplet merging, and splitting in a massively parallel fashion, which would be valuable for biological and chemical analysis.

This project is supported in part by NSF CAREER AWARD ECCS-0747950 and Institute for Cell Mimetic Space Exploration (CMISE) through NASA URETI program.

[1]K. T. Kotz, Y. Gu, and G. W. Faris, J. Am. Chem. Soc. **127**, 5736 (2005).
[2]R. D. Sun, A. Nakajima, A. Fujishima, T. Watanabe, and K. Hashimoto, J. Phys. Chem. B **105**, 1984 (2001).
[3]D. Beyssen, L. L. Brizouala, O. Elmazriaa, and P. Alnot, Sens. Actuators B **118**, 380 (2006).
[4]K. L. Wang, T. B. Jones, and A. Raisanen, J. Micromech. Microeng. **17**, 76 (2007).
[5]S. Park, C. Pan, T.-H. Wu, C. Kloss, S. Kalim, C. E. Callahan, M. Teitell, and P. Y. Chiou, Appl. Phys. Lett. **92**, 151101 (2008).
[6]M. G. Pollack, R. B. Fair, and A. D. Shenderov, Appl. Phys. Lett. **77**, 1725 (2000).
[7]H. Moon, S. K. Cho, R. L. Garrell, and C. J. Kim, J. Appl. Phys. **92**, 4080 (2002).
[8]P. Y. Chiou, H. Moon, H. Toshiyoshi, C. J. Kim, and M. C. Wu, Sens. Actuators A **104**, 222 (2003).
[9]P. Y. Chiou, Z. Chang, and M. C. Wu, J. Microelectromech. Syst. **17**, 133 (2008).
[10]H.-S. Chuang, A. Kumar, and S. T. Wereley, Appl. Phys. Lett. **93**, 064104 (2008).
[11]M. Vallet, B. Berge, and L. Vovelle, Polymer **37**, 2465 (1996).
[12]P. Y. Chiou, A. T. Ohta, and M. C. Wu, Nature (London) **436**, 370 (2005).
[13]A. T. Ohta, A. Jamshidi, J. K. Valley, H.-Y. Hsu, and M. C. Wu, Appl. Phys. Lett. **91**, 074103 (2007).
[14]J. M. Oh, S. H. Ko, and K. H. Kang, Langmuir **24**, 8379 (2008).
[15]S. H. Ko, H. Lee, and K. H. Kang, Langmuir **24**, 1094 (2008).